

Geotechnical characterization of the estuarine deltaic deposits in the Guayaquil city through in situ and laboratory tests

Bosco Intriago Álvarez¹ , Hernán Bazurto Palma¹ , Davide Besenon^{1#} ,
Xavier Vera-Grunauer² , Sara Amoroso^{3,4} 

Article

Keywords

Seismic dilatometer test
Piezocone test
Soft clays
Diatoms
Estuarine deltaic deposits
Geotechnical characterization

Abstract

According to previously available research and seismic microzonation studies a large area of the Guayaquil (Ecuador, South America) sits on estuarine deltaic deposits which consist of weak and highly compressible clays with diatoms. The nature of these fine-grained deposits may determine difficulties in a proper estimation of the soil properties. In this respect, the paper provides a detailed geotechnical and geophysical characterization of these soft clays, carried out in the estuarine complex of the Ecuadorean city. Borehole logs, standard penetration tests (SPT), piezocone tests (CPTu), a seismic dilatometer test (SDMT), a non-invasive geophysical survey, and laboratory tests were performed and then compared to analyze the static and dynamic geotechnical parameters of these deposits. The interpretation of the results highlighted the higher reliability of CPTu and SDMT rather than SPT and characterization lab testing to estimate soil shear strength, compressibility and stress history due to the soft nature of these clays, underlining also a certain sensitivity to the presence of the diatoms.

1. Introduction

Guayaquil is located on the West margin of the Guayas River along the Pacific coast of South America. Its soil deposits have been widely studied in the last decades due to the increasing urbanization this Ecuadorian city has experienced. Nevertheless, limited information is available in the literature on estimating geotechnical parameters related to this area.

The estuarine zone of the Guayas River deposits is highly heterogeneous. The soil stratigraphy consists of very soft, weak, and highly compressible sediment over hard rocks of Piñon and Cayo Formation (Vera-Grunauer, 2014). These soils present in their clayey matrix clay minerals including diatoms that result abundant in the upper 15-20 m depth of the Guayaquil deposits (Vera-Grunauer, 2014; Torres et al., 2018). The chemical composition of diatoms and their porous microstructure affect clay behavior, since the diatom skeletons or frustules contain a large number of voids or open pores, approximately between 60 and 70% according to Losic et al. (2007). These spaces allow great absorption of water, leading to a possible alteration of the soil properties.

Caicedo et al. (2018) established that for Bogota soils, diatoms increase the plasticity index (I_p), compromising the use of the Unified Soil Classification System (USCS)

(ASTM, 2017). Similarly, Shiwakoti et al. (2002) concluded that the Atterberg limits increase significantly due to the presence of diatoms. Besides, as long as the concentration of diatoms increases, the coefficients of compressibility and permeability also increase. Due to the minerals' rough surface and interlocking shape, the effective friction angle and shear strength rise too (Díaz-Rodríguez & González-Rodríguez, 2013).

For the above considerations it assumes relevance to study the soil behavior of these Ecuadorean soft soils, evaluating also that most methods or geotechnical correlations are calibrated on datasets that do not consider the diatom content in soft clays. A proper characterization of soil parameters requires an integrated approach whereby the geophysical method, in situ, and laboratory tests are used. However, data from geotechnical tests depend on many factors, including stress history, grain size, minerals, composition and packing of the particles. Consequently, a generalized correlation, consistent for some soil types, does not necessarily fit well for other geomaterials (Mayne, 2006).

In Ecuador, the standard penetration test (SPT) is overused for geotechnical design, considering the limited cost of execution during the cores, the usual availability of the SPT equipment, and its easy implementation. However,

#Corresponding author: E-mail address: besenon@espol.edu.ec

¹Escuela Superior Politécnica del Litoral, Facultad de Ingeniería en Ciencias de la Tierra, Guayaquil, Ecuador.

²Geostudios S.A., Guayaquil, Ecuador.

³University of Chieti-Pescara, Department of Engineering and Geology, Pescara, Italy.

⁴Istituto Nazionale di Geofisica e Vulcanologia, L'Aquila, Italia.

Submitted on August 5, 2021; Final Acceptance on June 3, 2022. Discussion open until November 30, 2022.

<https://doi.org/10.28927/SR.2022.074021>

 This is an Open Access article distributed under the terms of the Creative Commons Attribution License, which permits unrestricted use, distribution, and reproduction in any medium, provided the original work is properly cited.

its use should not be generalized to all soils, especially to soft clays (Stroud, 1988). Besides, the samples obtained are highly altered, and therefore not representative of the in-situ conditions (Mayne et al., 2009). In this respect, it is advisable, as recommended by Mayne et al. (2009), to use direct push in situ tests, such as the piezocone test (CPTu) and the seismic dilatometer test (SDMT), fast and very convenient for routine site investigations, to better capture the undrained and drained behavior of cohesive and incoherent soils, respectively. This paper aims to provide a scientific contribution to the limited subsoil information available in the literature for the Ecuadorian city of Guayaquil, supplying a detailed geotechnical and geophysical characterization of the estuarine deposits, composed by soft clays with diatoms. The results of the in situ and laboratory tests are presented and compared to verify the use of the different geotechnical tests and correlations for these diatom rich fine-grained sediments.

2. Site investigation

2.1 Geological settings

Ecuador is considered a country with high seismic risk due to its location on an active subduction tectonic margin with direction N80°E (Benítez, 1995; Benítez et al., 2005; Egüez et al., 2003), where the Nazca plate collides

and subducts with the Continental segment formed by the Northern Andean block and the Southern American plate (Chunga et al., 2019).

The study area of Guayaquil city, in the Kennedy Norte sector, is located in the Ecuadorian coastal region with an average ground surface level of 3.3 m above mean sea level (Figure 1). This area presents different geological formations, where the three main representative geological units are known as Guayaquil, Cayo, and Piñon formations. Guayaquil Formation is mainly constituted by siliceous shales, Piñon Formation is associated with siliceous sediments and Cayo Formation is characterized by intra-oceanic volcanic arc sequences (Benítez, 1990; Benítez et al., 2005; Salocchi et al., 2020). These geomorphological features of Guayaquil support the convergence of three macro-geological domains: alluvial plain of the Daule and Babahoyo rivers; Chongón-Colonche Cordillera hills and the estuarine deltaic complex of the Guayas River. This latter complex (later defined also as lithological unit D3) results composed by very soft and highly compressible deposits that, once analyzed microscopically, show in their clayey matrix minerals of heterogeneous composition.

Diatoms are one of these components and, as reported by Vera-Grunauer (2014), in the Kennedy Norte area their content fluctuates between 5.6 million per gram of soil to 1.4 million per gram in the upper 15-20 m, being less at greater

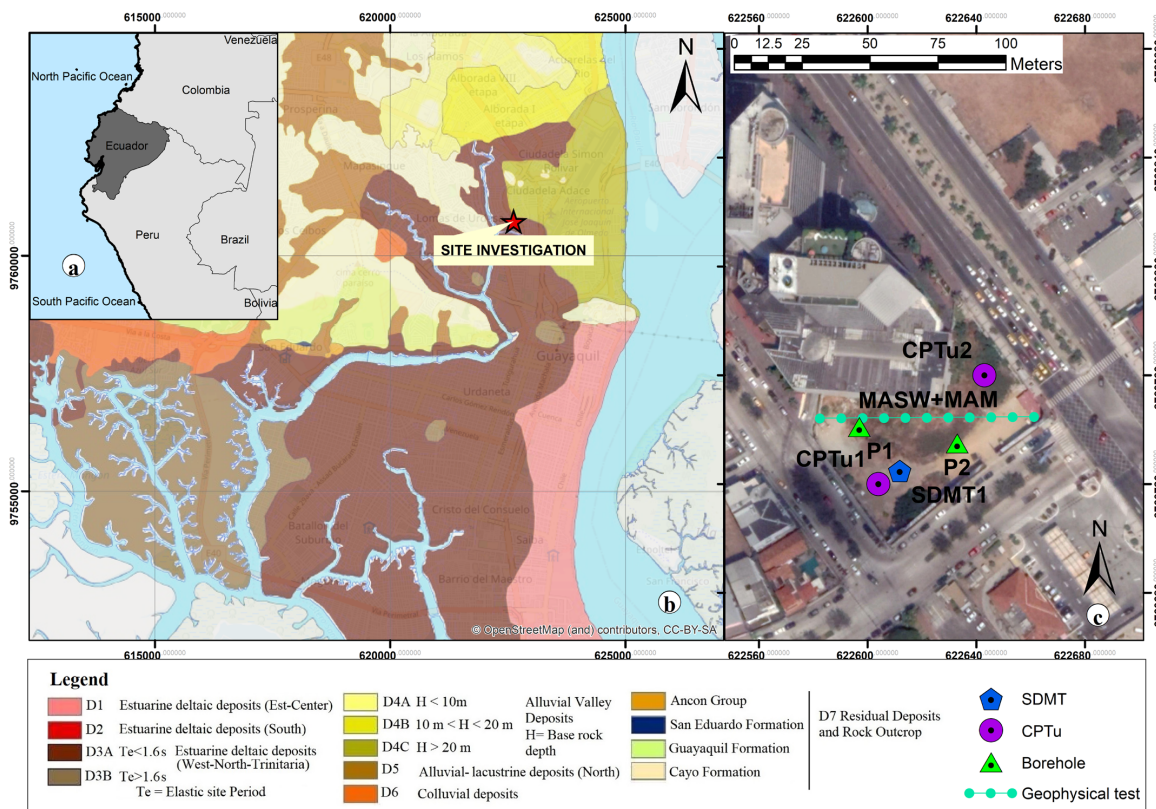


Figure 1. (a) location of the test site (a); (b) geological map of the study area; (c) location of the investigations at the Murano site.

depth. The diatom species with the highest abundance are *Thalassiosira*, *Actinocyclus*, *Stephanopyxis*, *Chaetoceros*, *Cyclotella*, *Coccosinodiscus*, *Actinopterychus*, *Rhaphoneis*, *Cocconeis*, and *Diploneis* spp., that correspond mostly to centric diatoms (Vera-Grunauer, 2014). The abundance of diatoms could be related to the extremely high number of volcanoes of the Ecuadorian region (Vera-Grunauer, 2014). Figure 2 shows the microstructure identified in the estuarine deltaic deposit of Guayaquil.

A seismic microzonation study is also available for Guayaquil, classifying the city into seven lithological units (Figure 1b; Vera-Grunauer, 2014). The study area of this research is Murano, located in the Kennedy Norte sector (North-East of the city), along two estuarine branches of the Guayas River, and characterized by soft sediments with a relevant diatom content in the upper 15–20 m depth (Vera-Grunauer, 2014; Torres et al., 2018). According to the microzonation map the Murano site corresponds to the lithological unit D3, defined as Holocene estuarine deltaic deposits.

2.2 Description of the site campaign

Multiple geotechnical and geophysical surveys were carried out to reconstruct a more accurate subsoil characterization at the Murano site (Figure 1c, Table 1). The investigation included two boreholes, with SPTs and retrieval of disturbed samples for soil classification, two piezocones, one seismic dilatometer including dissipation

tests and one multichannel analysis of surface waves (MASW) survey with one microtremor array measurement (MAM). The undisturbed samples were not herein considered since, according to Lunne et al. (1997) criterion, the quality of these samples was in general classified as poor to very poor.

2.3 Direct and intermediate measurements

Figure 3 summarizes the results of the direct and intermediate measurements obtained from the in situ geotechnical and geophysical investigations: for SPT, the SPT blows counts (N_{SPT}); for CPTu, the corrected cone resistance (q_t), sleeve friction (f_s), and pore water pressure (u_2); for the SDMT, the two corrected pressure readings, namely p_0 (1st reading) and p_1 (2nd reading), the horizontal stress index (K_D) and the shear wave velocity (V_s). The low N_{SPT} and q_t measurements and the high f_s and u_2 values in the upper 30 m of depth, together with the proximity of p_0 and p_1 pressures depth by depth, agree to identify the profile of a soft and clayey soil preliminarily. As shown in Figure 3, CPTu and DMT direct parameters increase quite gradually with depth, while the N_{SPT} profile show clearly a layer change at about 10 m depth. Moreover, for DMT, one measurement for the 3rd corrected pressure reading (p_2) is available and equal to 135 kPa in a thin sandy layer located at 17 m of depth. According to Marchetti et al. (2001), p_2 values are generally used to estimate the hydrostatic pore water pressure (u_0) in incoherent deposits. Therefore, the ground water level (GWT) can be estimated at 3.24 m of depth at the

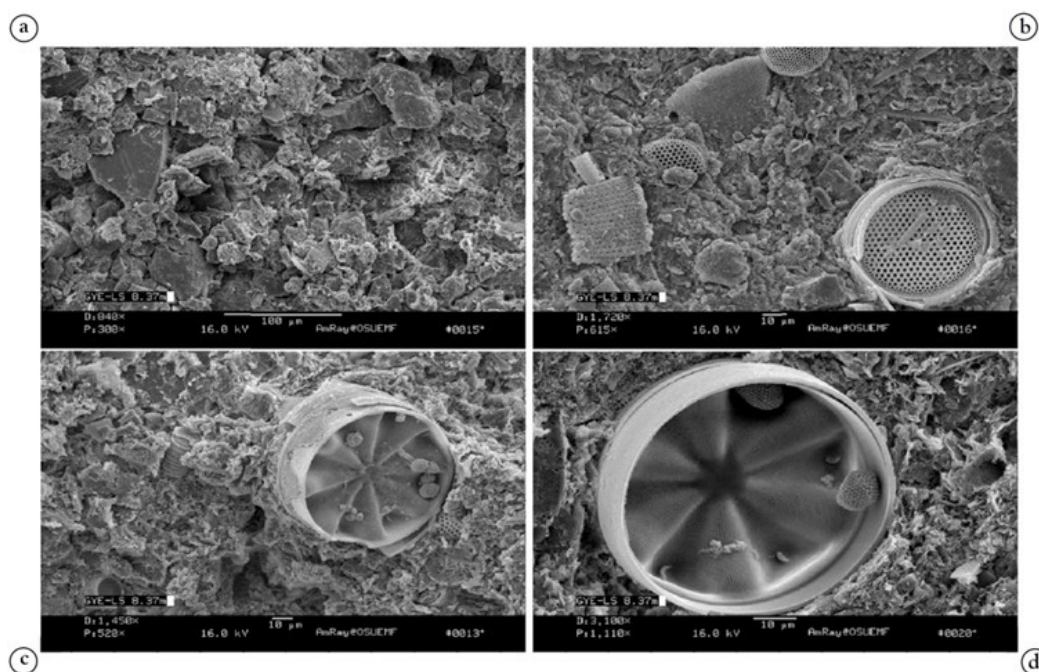
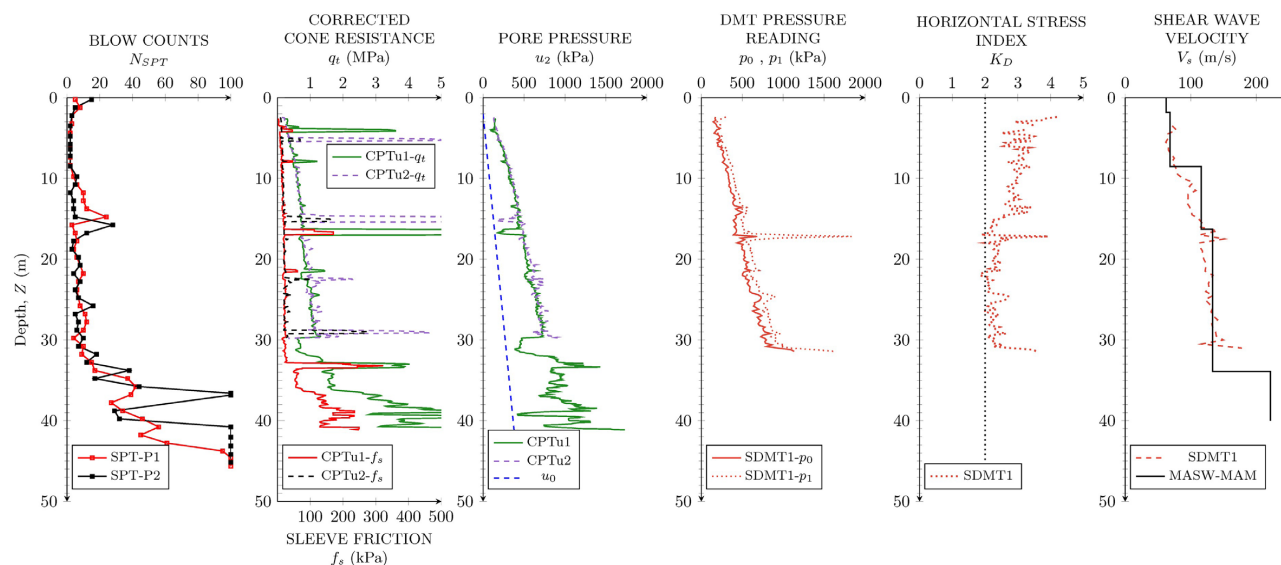


Figure 2. Scanning electron micrographs of Kennedy Norte sediment: (a) Sample with thin sand lamina; (b) silty clay with diatoms and diatom fragments; (c) diatomaceous smectite-rich clay matrix surrounds larger very fine sand-size diatoms; (d) well preserved diatom skeleton with micropores (<0.5 mm) (Vera-Grunauer, 2014).

Table 1. Summary of the field investigations performed at the Murano site.

Field test	Depth ¹ (m)	Dissipation test depth (m)	Disturbed samples	SPT per borehole	GWT depth (m)	Test date
P1	46.00	-	45	45	1.80	14/11/2018
P2	45.00	-	45	45	2.00	08/11/2018
CPTu1	41.00	10.60; 13.45	-	-	2.05	12/11/2018
CPTu2	30.00	8.00; 12.00	-	-	1.82	09/11/2018
MASW+MAM	80.50	-	-	-	-	-
SDMT1	31.40	8.00	-	-	3.24	05/08/2018

¹ For MASW+MAM survey, the value corresponds to receiver spread length.


Figure 3. Measured parameters for geotechnical and geophysical tests at the Murano site.

DMT test site. The CPTu test can also be used to estimate the GWT through u_2 in the thin sandy layers; in this case, GWT is at about 2.05 m for CPTu1 and 1.82 m for CPTu2. For boreholes P1 and P2, GWT was measured at 1.80 and 2.00 m of depth respectively. CPTu tests and boreholes were performed roughly in the same wet period (Table 1), which justifies the good agreement between GWT results. On the contrary, SDMT1 was conducted in the Ecuadorian dry season, explaining the GWT variation due to seasonal fluctuations. In addition, despite Guayas River and its Estuarine Complex are influenced by sea level fluctuations, tidal variation should not influence the GWT level due to the low permeability of these fine-grained deposits.

The K_D profile shown in Figure 3 gives information on the stress history of the deposits (Marchetti, 1980):

$$K_D = (p_0 - u_0) / \sigma'_{v0} \quad (1)$$

where the hydrostatic pore water pressure (u_0) is obtained using the GWT profile estimated from DMT and the vertical effective stress (σ'_{v0}) is estimated from DMT using the soil

unit weight (γ) by Marchetti & Crapps (1981) chart. The complete γ profile is provided in the subsequent section.

As shown in Equation 1, K_D can be regarded as an amplified in situ coefficient of earth pressure at rest (K_0) since $(p_0 - u_0)$ is an “amplified” horizontal effective stress (σ'_{h0}) due to penetration. According to Marchetti et al. (2001) the horizontal stress index K_D is noticeably reactive to stress history, prestraining/aging and structure, scarcely felt by q_t from CPT. In normally consolidated (NC) clays, usually identified with an overconsolidation ratio $OCR \approx 1$, the value of K_D is approximately equal to 2, and this justifies that the K_D profile is similar in shape to the OCR profile (Jamiolkowski et al., 1988). At the Murano site the K_D profile provides a value of $K_D \approx 3$ within the upper 15 m, and of $K_D \approx 2$ in the bottom layer (15-30 m) that can be associated to a NC behavior. The higher K_D values revealed in the upper 15 m can be associated to the stress history of this layer and potentially to a “structure-induced overconsolidation” (i.e. “apparent overconsolidation”), representing the Guayaquil diatomaceous naturally cemented clays. As documented by Vera-Grunauer (2014) and Torres et al. (2018), this sediment seems to have a greater proportion of diatomaceous

material and may initially have had a higher organic matter content. This resulted in local cementation of the sediment by framboidal pyrite.

Finally, the SDMT- V_s profile is compared to the MASW+MAM- V_s interpretation, highlighting a good agreement between the geophysical and geotechnical methods. The passive measurements also provide an ambient noise curve, detecting a peak frequency at 0.796 Hz, which corresponds to an elastic period $T_e = 1.256$ s. This value correctly matches the seismic microzonation study (Vera-Grunauer, 2014) that identifies the Murano area as a D3A zone, namely estuarine deltaic deposits with $T_e < 1.6$ s.

Other direct measurements obtained at the site are related to CPTu and DMT dissipation tests, as for the coefficient of consolidation in horizontal direction (c_h) (Robertson et al., 1992; Marchetti & Totani, 1989). Figure 4a shows the results of the CPTu pore water pressure (u_2) with time (t) together with the points corresponding to the measured time for the 50% of dissipation (t_{50}). Figure 4b illustrates the profile of the non-corrected 1st DMT reading (A) with the time (t) in combination with the contraflexure point of the curve (t_{flex}). The c_h values obtained by dissipation tests are equal to $4.20 \cdot 10^{-6}$ and $5.20 \cdot 10^{-6}$ m²/sec for CPTu1 and to $1.70 \cdot 10^{-6}$ and $1.40 \cdot 10^{-6}$ m²/sec for CPTu2, assuming a value of the rigidity index equal to 70 according to Mayne (2007). The c_h value obtained in the clayey layer by DMT is equal to $2.6 \cdot 10^{-5}$ m²/sec.

3 Geotechnical characterization of the test site using in situ and laboratory tests

3.1 Soil classification

Laboratory and in situ testing were analyzed to obtain a detailed soil classification. Figure 5 shows the borehole log using USCS soil classification (ASTM, 2017), the soil

composition, the Atterberg limits (liquid limit w_L , plastic limit w_p), the plasticity index (I_p), the water content (w) and the liquidity index (I_L), the CPT soil behavior type index (I_c) and the DMT material index (I_D). The water content was considered as a minimum value, due to the possible changes of the natural conditions of the collected SPT disturbed samples. However, the use of the SPT Raymond sampler provided the advantage to have a quite continuous profile of the index laboratory parameters (i.e. w_L , w_p , I_p , w , I_L), detecting any eventual sudden change in the stratigraphy (Stroud, 1988).

Although the liquidity index values are not usually presented in percentage, this is herein done just to show the liquidity index values in Figure 5 along with the other physical indexes. The soil stratigraphy is apparently quite uniform up to approximately 33-37 m, showing mainly clays with high plasticity (mean $I_p > 40\%$), liquidity index (mean $I_L > 120\%$) and liquid limit (mean $w_L > 70\%$). In particular, from 0 to 15 m, the predominance of silt and clay soil is observed, characterized by an average I_p of 46% and w of about 86%. The cohesive deposits continue to prevail from 15 to 30-37 m, but the percent of sand starts to increase and the I_p and w values decrease, staying in a range of 30-50% and 70-90%, respectively. Below 30-37 m of depth, the percentage of sand continues to increase up to 60%, and also a relevant presence of gravel (37-54%) is encountered. Consequently, Atterberg limits and water content values decrease. A first order estimate of the void ratio may be also obtained from w assuming the soil in saturated conditions. Thus, for a given specific gravity value ($G_s = 2.67$), determined via laboratory tests, and the water content profile obtained from SPT retrieved samples, the void ratio value is approximately equal to 2.36 up to 15 m and to 2.10 between 15 and 32 m. The large void ratio is probably due to process of “clay bonding”, since the clay particles of the Guayaquil deltaic estuarine deposits may adhere to the large surface of diatoms, as reported by Vera-Grunauer (2014).

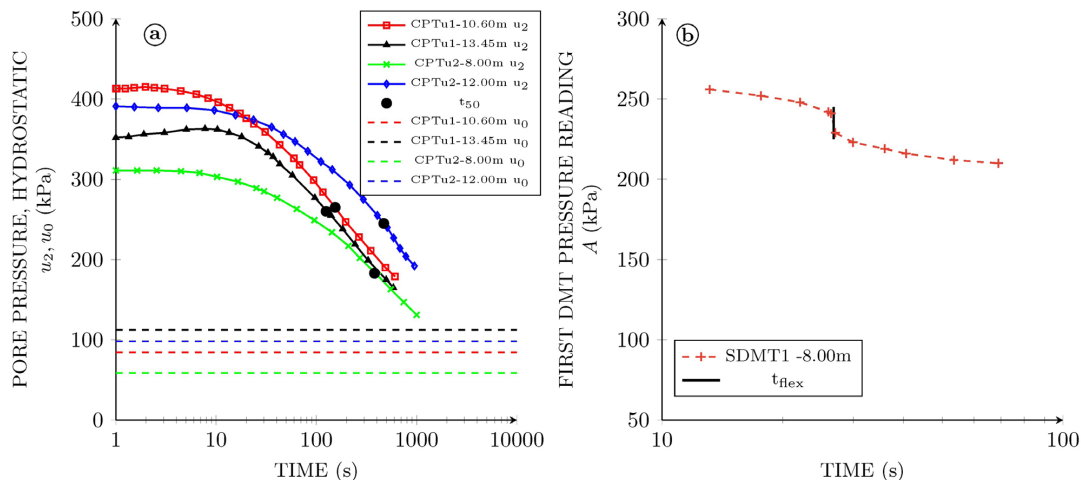


Figure 4. Dissipation tests from: (a) CPTu tests; (b) DMT test.

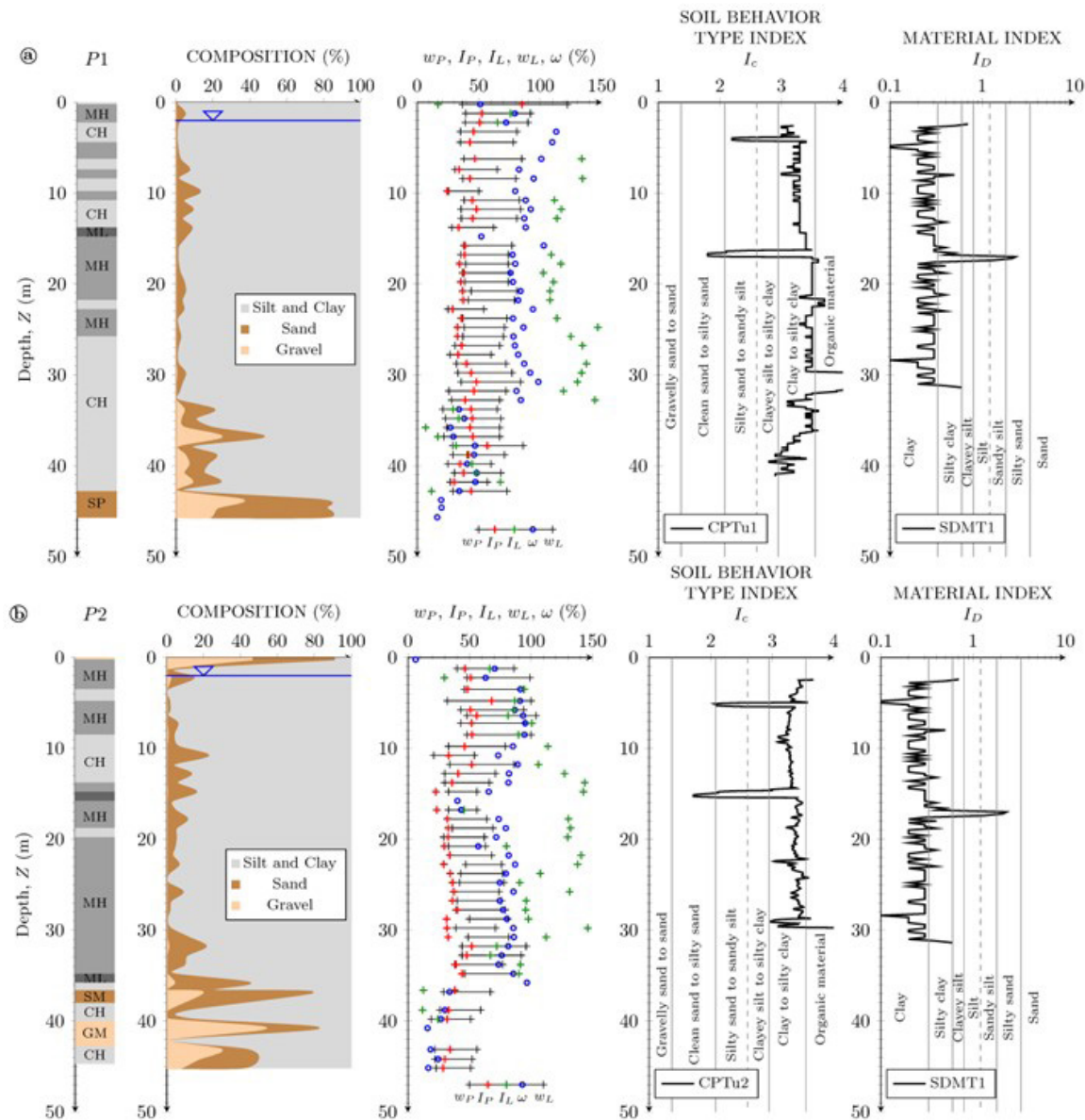


Figure 5. Soil classification using USCS method, CPTu and DMT interpretations, soil composition and basic properties for boreholes: (a) P1; (b) P2.

The I_c and I_D profiles, estimated using Robertson & Cabal (2015) and Marchetti et al. (2001) respectively, are in broad agreement with the soil stratigraphy obtained from the boreholes and the lab testing, since in situ tests detect on average a clay layer up to 40 m depth with a thin silty sand lens between 15 and 17 m depth. However, there is no perfect correspondence between the CPT-DMT geotechnical description and the grading curves (i.e., soil composition percent), since both I_c and I_D are parameters related to the mechanical soil response and not strictly to the grain size distribution of the soil deposits (e.g.: Boncio et al., 2020). The integrated information of gradations and index properties may find better agreement with the I_c and I_D values. For example,

correspondence to low-plastic deposits by P2 (Figure 5b) is noticed for the silty sands detected by CPTu2 at about 15 m.

Finally, it can be observed that for most of the soil samples within the upper 30-37 m depth, w is generally higher than 70%, recording also values bigger than 100%. Particularly, the highest I_p , w_L , w_p and w values are concentrated in the upper 15 m depth. This information is in line with the results by Vera-Grunauer (2014), who performed scanning electron micrographs for soil samples taken at sites close to the studied area. Vera-Grunauer (2014) observed that the microporous structure of diatoms consisted of open pores with a diameter less than 0.5 μm which generates a large specific surface and allows the absorption of a large amount of water.

As described by Díaz-Rodríguez & González-Rodríguez (2013) and Caicedo et al. (2018) for the Mexico City and Bogota clays, the increment in diatom content raises the liquid limit and water content. Therefore, it is probable that the high values of the water content in the upper 15 m depth could be explained by the high presence of the diatoms, as mentioned above.

3.2 Strength and compressibility

The total unit weight (γ) is an important parameter because it indirectly shows an idea of the field state of soil stress at any desired depth (Rodríguez et al., 2015). Recommended γ values were proposed by Look (2007) for cohesive soils, from soft organic with $\gamma \approx 14 \text{ kN/m}^3$ to soft non-organic with $\gamma \approx 16 \text{ kN/m}^3$ and, to stiff to hard with γ between 18 to 20 kN/m^3 . Robertson & Cabal (2015) determined that the unit weight values are in direct proportion of q_t and the friction ratio R_f , with values around 12.5 kN/m^3 for organic material and 17.5 kN/m^3 for clays. Moreover, Mayne (2016) established a direct relationship between γ and f_s , for an average value of 17.5 kN/m^3 in clays and 13.5 kN/m^3 in diatomaceous mudstone.

At the Murano site the γ profiles obtained from CPTu and DMT interpretations (Figure 6), according to Robertson & Cabal (2015) and Marchetti & Crapps (1981) charts respectively, provide unit weight values that increases with the depth into the homogeneous clay from 14 to 17 kN/m^3 , due to increased effective vertical stress (σ'_{v0}). Actually, soil unit weights should be obtained by intact samples. The main scope of CPTu and DMT charts is not an accurate estimation of γ , but the possibility of constructing an approximate

σ'_{v0} profile, needed in the interpretation of in situ tests (Robertson & Cabal, 2015; Marchetti et al., 2001).

Undrained shear strength (s_u) coupled with total stress analysis is often used to examine the failure state of geotechnical structures under undrained conditions in Guayaquil City (Vera-Grunauer, 2014). At the Murano site, Brown & Hettiarachchi (2008), Robertson (2010) and Marchetti (1980) correlations were used to estimate s_u from SPT, CPTu and DMT, respectively, although SPT is suited for the use in evaluating strength and compressibility of loose to dense granular soils, with extended applications to stiff to hard clays and silts (e.g. Stroud, 1988; Mayne et al., 2009). CPTu and DMT give similar profiles, while SPT provides lower values within the upper 20 m depth, moving closer to DMT and CPTu prediction at greater depth (Figure 6).

Penetration test results are most commonly used to estimate the soil settlement, using the constrained modulus (M), which depends on the stress state, soil type, and overconsolidation ratio. These dependencies are incorporated into CPT and DMT empirical correlations since M from CPT (Robertson, 2009) is related to the I_c and the in situ vertical stress, and M from DMT (Marchetti, 1980) is a function of the I_D , of the K_D and of the dilatometer modulus (E_D). The in-situ predictions are still in close agreement with each other between 7 and 15 m depth ($M \approx 2.5 \text{ MPa}$), while at greater depths, DMT always provides higher values compared to CPT (Figure 6). According to the numerous case histories available in the literature (e.g., Monaco et al., 2014; Monaco & Calabrese, 2006; Schmertmann, 1986, 1988; Mayne, 2005; Berisavljević, 2017), usually the measured settlements are in good agreement with the DMT-predicted values thanks to the high reliability of the DMT constrained modulus M , a working strain modulus. M by DMT is therefore associated

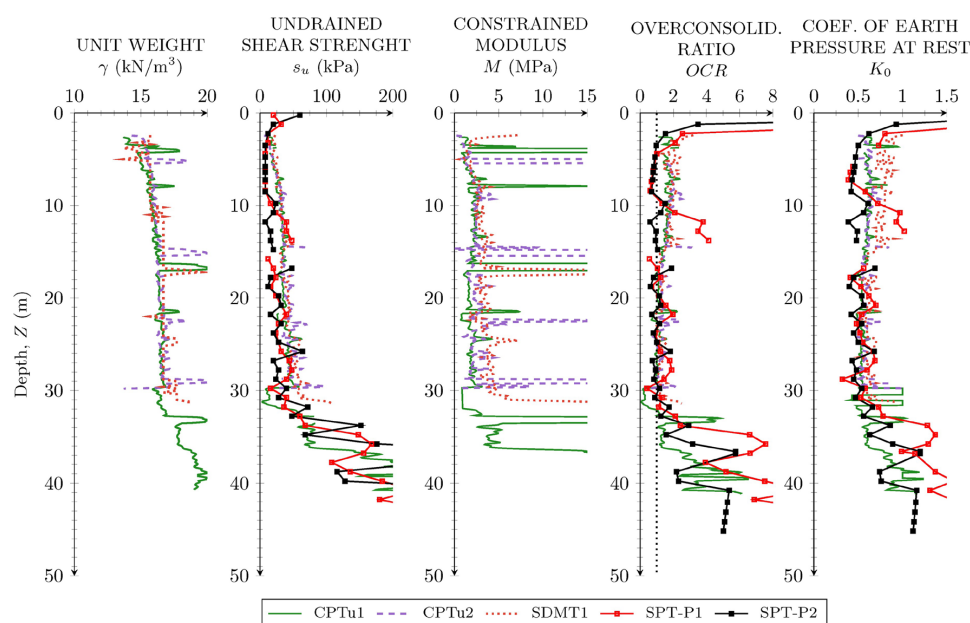


Figure 6. Geotechnical parameters estimated from laboratory and in situ tests.

with an intermediate strain level, more appropriate for the settlement calculations. In contrast, penetration tests, like CPT, working at higher strains due to the considerable distortion induced by the CPT conical tip, produce a less reliable M estimation (Baligh & Scott, 1975; Mayne, 2001).

For evaluating the overconsolidation, the abovementioned strong dependence between K_D and stress history in clay supported the use of DMT to obtain a more reliable estimate of OCR , using the Marchetti (1980) formula, rather than from CPT and SPT. However, the OCR predictions of fine-grained soils were also provided for CPT, using the normalized q_t values (Kulhawy & Mayne, 1990), and for SPT, using SHANSEP approach and site parameters, selected for the D3 estuarine deltaic zone of Guayaquil (Vera-Grunauer, 2014). A good agreement was shown between CPT and DMT for the entire profile, estimating $OCR \approx 2$ within the upper 15 m and a value of $OCR \approx 1$ (or slightly higher than 1) approximately between 15 and 30 m. This confirms the behavior preliminarily observed in the K_D profile (see Figure 3), being potentially due to the “apparent overconsolidation” of the diatomaceous naturally cemented Guayaquil clays.

For the estimation of the coefficient of earth pressure at rest (K_0), the use of pressurimeter and/or flat dilatometer tests is recommended by the literature (e.g., Mayne et al., 2009), considering they can be considered as “horizontal-expansion” tests. Specifically, for the DMT the horizontal stress index (K_D), having been regarded as an amplified K_0 (see Equation 1), can provide reliable estimates in clayey deposits by a correlation obtained experimentally by Marchetti (1980), and later theoretically by Yu (2004):

$$OCR = (0.5 \cdot K_D)^{1.56} \quad (2)$$

Estimates of K_0 can be also provided by CPT and SPT tests for low plastic fine-grained soils, using the OCR values estimated by each own test (Kulhawy & Mayne, 1990), as follow:

$$K_0 = 0.5 \cdot OCR^{0.5} \quad (3)$$

However, the “weak” dependency of SPT and CPT from the stress history together with the considerable scatter in the CPT and SPT database used to determine OCR and K_0 can only provide an order of magnitude of these parameters (Robertson & Cabal, 2015).

The comparison of K_0 profiles, shown in Figure 6, provides $K_0 \approx 0.8$ by DMT in the upper 15 m depth and lower values by SPT and CPT, while K_0 estimations by all the in-situ tests are consistent at greater depth, providing an average NC value of 0.6 between 15 and 30 m depth. This difference between the geotechnical behavior of the upper 15 m-thick layer and the lower 15 m-thick layer, as detected

by K_D , OCR , K_0 and index parameters (w_L , w_p , I_p , w), may be potentially interpreted as a different concentration of diatoms, higher in the top layer than in the bottom. This assumption finds a consistency with the analyses of Vera-Grunauer (2014) and Torres et al. (2018) that in the Guayaquil estuarine complex revealed the abundant presence of diatoms in the upper 15-20 m depth.

3.3 Permeability

In situ tests were also used to determine permeability. Robertson (2010) developed a correlation between I_c and the coefficient of permeability (k) to obtain an entire but approximate permeability profile that is not sensitive to the anisotropy of the soil. However, better estimation of the horizontal permeability (k_h) can be provided by dissipation tests from both CPTu and DMT. Teh & Houslyby (1991), Perez & Fauriel (1988) and Robertson (2010) relationships were used for CPTu tests, once t_{50} , and consequently c_h , were estimated from dissipation curves (Figure 4). These three correlations provide similar values, and therefore for clarity in Figure 7 only Robertson (2010) estimation is shown. Similarly, for DMT test t_{flex} and c_h were used to estimate k_h according to Marchetti & Totani (1989).

The results obtained at the Murano site show that in the layer at 8.00 m depth horizontal permeability k_h obtained from DMT1 dissipation tests ($k_h \approx 10^{-7}$ m/s, silty clay with $I_D = 0.21$) is one order magnitude higher than k_h from

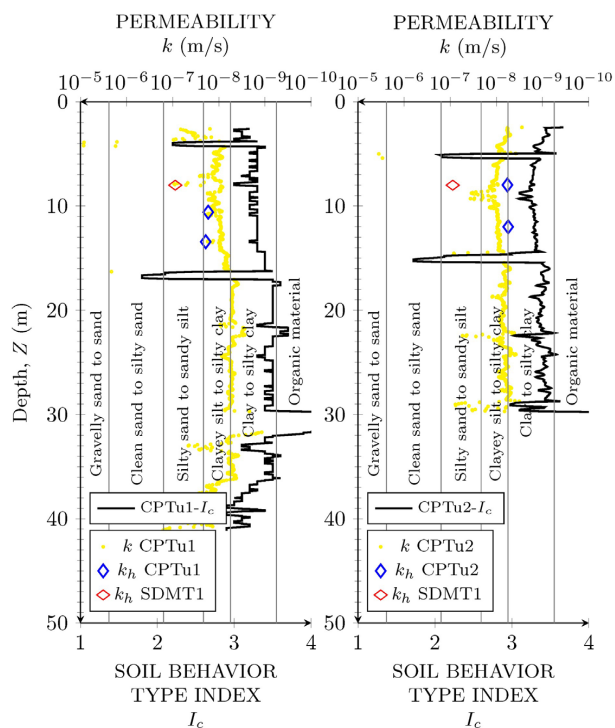


Figure 7. Permeability estimates together with soil behavior index profiles for CPTu1 and CPTu2.

CPTu2 (clay to silty clay with $I_c = 3.29$). The continuous k profile derived from I_c has been found in broad agreement with the results of CPTu dissipation tests at the Murano site. Higher permeability is encountered in sandy soils ($k_h \approx 10^{-6}$ m/s) while lower values are confined to soft clay ($k_h \approx 10^{-8}$ m/s, slightly lower between 15 and 30 m depth) in reasonable agreement with permeability ranges obtained by Holtz et al. (1981). Probably, the higher horizontal permeability for the upper 15 m depth is related to its higher diatom content, when compared to the lower layer.

4. Dynamic soil properties at the test site using geotechnical and geophysical measurements

4.1 Shear wave velocity

The estimation of the shear wave velocity (V_s) is fundamental in geotechnical engineering design, not only for site classification and soil-structure interaction, but also for earthquake analysis and site response. Penetration tests can be used for predicting V_s through some measured parameters. In particular, DMT allows to estimate the small strain shear

modulus (G_0), based on the intermediate parameters I_D , K_D , M (Marchetti et al., 2008):

$$G_0 = M \cdot 26.177 \cdot K_D^{-1.0066} \text{ for clays } (I_D \leq 0.6) \quad (4)$$

$$G_0 = M \cdot 15.686 \cdot K_D^{-0.921} \text{ for silt } (0.6 < I_D < 1.8) \quad (5)$$

$$G_0 = M \cdot 4.5613 \cdot K_D^{-0.7967} \text{ for sands } (I_D \geq 1.8) \quad (6)$$

V_s can be then obtained referring to the theory of elasticity:

$$V_s = \sqrt{G_0 / \rho} \quad (7)$$

Where ρ is the density of the soil that can be calculated from the unit weight determined by Marchetti & Crapps (1981) chart at each depth.

Several authors have developed and recommended correlations for SPT, expressed as a function of N_{SPT} , N_{60} , depth (Z), soil type and geological age (Table 2). Finally, for CPT several correlations are available to predict V_s , that are

Table 2. Main available equations to estimate V_s from SPT.

Author	Soil Type ²	V_s correlation	Geological description
Wair et al. (2012)	All soils	$V_s = 26 \cdot N_{60}^{0.215} \cdot \sigma'_{v0}^{0.275}$	Holocene
	All soils	$V_s = 34 \cdot N_{60}^{0.215} \cdot \sigma'_{v0}^{0.275}$	Pleistocene
	Clays and silts	$V_s = 23 \cdot N_{60}^{0.17} \cdot \sigma'_{v0}^{0.32}$	Holocene
	Clays and silts	$V_s = 29 \cdot N_{60}^{0.17} \cdot \sigma'_{v0}^{0.32}$	Pleistocene
	Sands	$V_s = 27 \cdot N_{60}^{0.23} \cdot \sigma'_{v0}^{0.23}$	Holocene
	Sands	$V_s = 35 \cdot N_{60}^{0.23} \cdot \sigma'_{v0}^{0.25}$	Pleistocene
Imai & Yoshimura (1970)	All soils	$V_s = 76 \cdot N_{SPT}^{0.33}$	-
Kalteziotis et al. (1992)	All soils	$V_s = 76.2 \cdot N_{SPT}^{0.24}$	-
	Sands and silts	$V_s = 49.1 \cdot N_{SPT}^{0.502}$	-
	Clays	$V_s = 76.55 \cdot N_{SPT}^{0.445}$	-
Ohsaki & Iwasaki (1973)	All soils	$V_s = 81.4 \cdot N_{SPT}^{0.39}$	-
	Sands	$V_s = 59.4 \cdot N_{SPT}^{0.47}$	-
Iyisan (1996)	All soils	$V_s = 51.5 \cdot N_{SPT}^{0.516}$	Deep alluvial deposits
Jinan (1987)	All soils	$V_s = 116.10 \cdot (N_{SPT} + 0.32)^{0.202}$	Soft Holocene deposits
Dikmen (2009)	All soils	$V_s = 58 \cdot N_{SPT}^{0.39}$	Quaternary alluvium
	Sands	$V_s = 73 \cdot N_{SPT}^{0.33}$	Quaternary alluvium
	Clays	$V_s = 44 \cdot N_{SPT}^{0.48}$	Quaternary alluvium
	Silt	$V_s = 60 \cdot N_{SPT}^{0.36}$	Quaternary alluvium

² For groups of formulas, the best used is highlighted.

related to numerous parameters like tip resistance (cone tip resistance q_c or corrected cone tip resistance q_t, f_s), confining stress, Z , soil type, and geologic age (Table 3).

Figure 8a provides the comparison between V_s measured (MASW+MAM and SDMT) and V_s predicted by DMT (Marchetti et al., 2008), that shows a reasonable agreement. There is a slight overestimation of DMT predicted values, more pronounced in the upper 15 m that could be related to the higher concentration of the diatoms as previously detected by K_D (through K_0 and OCR) that is noticeable more reactive to stress history, structure and prestraining/aging, scarcely felt by the cone resistance q_c (or the corrected cone resistance q_t) from CPT (Amoroso, 2014). A large number of correlations have been developed for SPT, involving the soil type, the geological description, and sometimes the in-situ stress. This results in a wide variability (Figure 8b) within the V_s profiles, as previously noted by other authors in different sites (e.g.: Fabbrocino et al., 2015; Akin et al., 2011). This is confirmed also for the soft clay deposits of Murano test site (Figure 8b, e.g.: Jinan, 1987) where, the estimated values are up to two times higher than the measured ones.

Similar behavior (Figure 8c) is observed with the V_s correlations developed for CPT test. This is confirmed also by Robertson (2012) that estimates values up to four times the measured ones. The arisen uncertainty could be due to the dependency to numerous and different parameters mentioned above that CPT and SPT parameters may not

capture correctly. However, it is possible to select the best SPT-Vs and CPT-Vs predictions for soft clay deposits using the formulas proposed by Wair et al. (2012), Dikmen (2009) and Kalteziotis et al. (1992) for SPT test (Figure 8d). Interestingly, the last two equations developed for all types of soils are in better agreement with the measured Vs profile than those made exclusively for clays. The selected Wair et al. (2012) equation is valid for Holocene clays and silts. For CPT test, Bouckovalas et al. (1989) and Vera-Grunauer (2014) resulted to fit better with V_s measurements, and they are valid for very soft clays and for clays with diatoms, respectively (Figure 8c). In particular, Vera-Grunauer (2014) proposed a site-specific correlation for the D3 estuarine deltaic zone of Guayaquil. All together the measured (SDMT, MASW+MAM) and selected-predicted (Marchetti et al., 2008; Wair et al., 2012; Dikmen, 2009; Kalteziotis et al., 1992; Bouckovalas et al., 1989; Vera-Grunauer, 2014) Vs data presented reasonable agreement identifying Vs values increasing in the 30 m depth in range of 50-180 m/s.

4.2 Stiffness decay curves

Finally, in situ tests were used to evaluate stiffness decay curves (G - γ curves). In particular, this opportunity is offered by SDMT that allows to estimate the in-situ variation of soil stiffness with the level of deformation, as preliminarily suggested by Marchetti et al. (2008) and then

Table 3. Main available equations to estimate V_s from CPT.

Author	V_s (or G_0) correlation ³	Geological description
Robertson (2012)	$V_s = \alpha_{vs} \cdot (q_t - \sigma'_{v0})^{0.5} / p_a$; $\alpha_{vs} = 10^{0.55 \cdot I_c + 1.68}$	Holocene and Pleistocene soils, mostly uncemented
Hegazy & Mayne (1995)	$V_s = [10.1 \log(q_t) - 11.4]^{1.67} \cdot f_s / q_t \cdot 100$	All types of soils
Simonini & Cola (2000)	$G_0 = 49.2 \cdot q_c^{0.51}$	Sand, silt and silty clay of Venice Lagoon
Andrus et al. (2007)	$V_s = 2.27 \cdot q_t^{0.412} \cdot I_c^{0.989} Z^{0.033}$, <i>ASF</i> ; <i>ASF = 1.00</i> $V_s = 2.62 \cdot q_t^{0.395} \cdot I_c^{0.912} Z^{0.124}$, <i>SF</i> ; <i>SF = 1.12</i>	Holocene soils Pleistocene soils
Madiai & Simoni (2004)	$V_s = 140 \cdot q_c^{0.30} \cdot f_s^{-0.13}$ $V_s = 268 \cdot q_c^{0.21} \cdot f_s^{0.02}$ $V_s = 182 \cdot q_c^{0.33} \cdot f_s^{-0.02}$ $V_s = 172 \cdot q_c^{0.35} \cdot f_s^{-0.05}$	Holocene cohesive soils Holocene incoherent soils Pleistocene cohesive soils Pleistocene incoherent soils
Bouckovalas et al. (1989)	$G_0 = 28.0 \cdot q_c^{1.40}$	Very soft clays
Vera-Grunauer (2014)	$V_s = \sqrt{\eta \cdot q_c} e^{\alpha}$ $\alpha = [(3N_{kc} - 4) / 4] - [1 / (2\beta)]$; $\eta = 3g / [2N_{kc} \cdot \gamma_s \cdot (1 + \nu)]$	Clays with diatoms

³ Legend: see List of Symbols. For groups of formulas, the best used is highlighted.

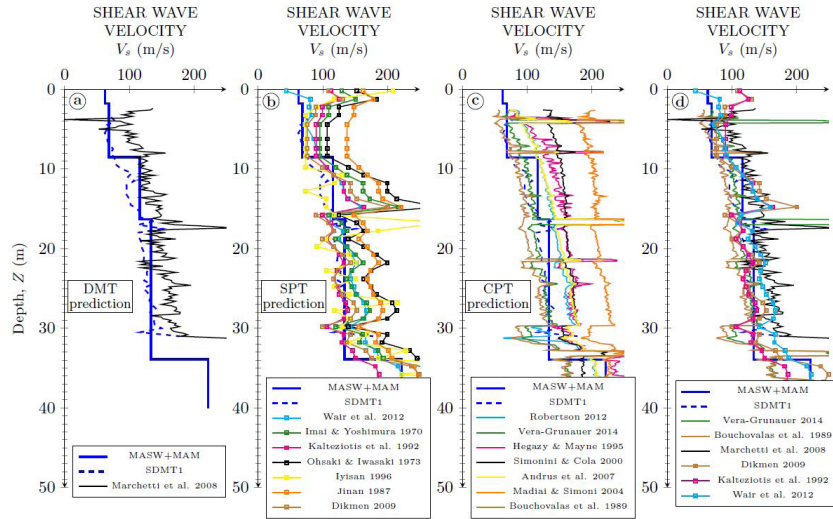


Figure 8. Comparison of V_s measured and V_s predicted by: (a) DMT; (b) SPT; (c) CPTu; (d) comparison of V_s measured and V_s predicted using the best correlations. The plots correspond to borehole P1, CPTu1 and SDMT1 tests.

tested by Amoroso et al. (2014) and Di Mariano et al. (2019). The method proposes firstly to assess the small strain modulus G_0 through the theory of elasticity using V_s .

Then it is necessary to evaluate a working strain shear modulus G_{DMT} starting from the constrained modulus (M also named M_{DMT}) obtained from the usual DMT test through the theory of elasticity:

$$G_{DMT} = M_{DMT} \cdot (1 - 2\nu) / [2 \cdot (1 - \nu)] \quad (8)$$

where ν = Poisson's ratio, assumed equal to 0.3 for all layers.

Amoroso et al. (2014) proposed an equation to determine a hyperbolic stress-strain equation to represent the non-linear soil behavior through a normalized decay curve ($G / G_0 - \gamma$ curve) by SDMT data:

$$G / G_0 = 1 / [1 + (G / G_{DMT} - 1) \cdot (\gamma / \gamma_{DMT})] \quad (9)$$

where G = shear modulus; γ = shear strain; γ_{DMT} = shear strain associated with the working strain DMT modulus for which Amoroso et al. (2014) suggested a range of values based on the soil type.

In this particular case, being Murano site composed by soft clays, it is recommendable to use a value of $\gamma_{DMT} = 2\%$. Moreover, to consider the effect of the confining stress and the different geotechnical properties of the entire soil profile into the assessment of the $G / G_0 - \gamma$ curves, seven homogeneous strata were identified from 3.50 to 31 m depth, as reported in Figure 9. The $G / G_0 - \gamma$ curves estimated in the upper 15.5 m have a similar behavior, while the deeper $G / G_0 - \gamma$ curves decay much faster. This aspect is related to the higher values of K_D , and hence of OCR and K_p , detected

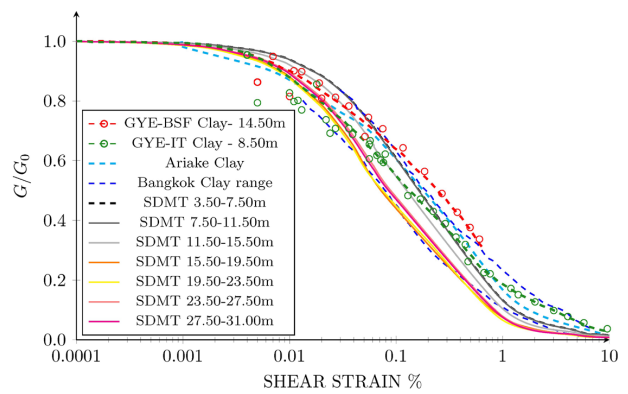


Figure 9. $G - \gamma$ decay curves for Guayaquil clays obtained by SDMT tests and comparison with results of laboratory curves.

for the upper layer, confirming a possible relationship with the different concentration of diatoms.

Figure 9 also plots two $G/G_0 - \gamma$ curves developed for Guayaquil clays in geological zone D3A whose samples were retrieved at Baseball Stadium Field (BSF-dashed red line), in the Kennedy Norte sector, on structure-induced OC diatomaceous clays and at Trinitaria Island (TI-dashed green line) on NC clays according to Vera-Grunauer (2014). The cyclic response of TI samples was evaluated by means of cyclic triaxial and simple shear tests while, for BSF clay, the decay curve was estimated from cyclic triaxial data. The conditions of the clay structure were modeled in the following way: to reproduce the conditions of the BSF clay, the recompression method was used during the consolidation stage and the SHANSEP procedure was applied to model the normally consolidated soil. As reported by Vera-Grunauer (2014), the lower decay of BSF clay is due to the influence of pyrite cementation in its soil fabric. Other laboratory curves are included in Figure 9 for naturally cemented alluvial

clays with diatoms: Bangkok clay (Teachavorasinskun et al., 2002) and Ariake clay (Nagase et al., 2006). A reasonable agreement is possible to detect by comparing the entire group of literature curves with $G/G_0-\gamma$ curves by SDMT. However, the best fitting can be found between Guayaquil (BSF) and Bangkok (upper limit) laboratory tests and SDMT prediction within the upper 15.5 m, probably due to the higher content of diatoms. Below that depth, SDMT assessment fits well with the lower limit of Bangkok clays.

5 Conclusions

The deep site campaign performed in Guayaquil (Ecuador) at the Murano site allowed to provide a better soil characterization for soft clays in presence of diatoms:

- Index properties looked to be potentially influenced by the diatom content: the microstructure and porous shape of diatoms increased the average I_p and w values in the upper 15 m depth, influencing the interpretation provided by USCS classification. This aspect is less visible from I_c (CPTu) and I_D (DMT);
- The parameters of resistance, compressibility and stress history provided reliable values in the Guayaquil clays using both CPT and DMT, while SPT usually detected lower values being not particularly effective in soft soils;
- The analysis of the OCR profiles by CPTu and DMT confirmed an apparent overconsolidation in the upper 15 m ($OCR \approx 2$) that could be explained by the presence of pyrite cementation in soil structure. This type of mineralogy is typical of marine environments; the main factor for the production of the cementing agent is the bacterial reduction of sulfate which is closely linked to the presence of diatoms. Similar observations emerged from K_D (and K_θ) values obtained only by DMT: K_D decreases from 3 to 2 moving from the upper 15 m to the lower layer, while K_θ decreases from 0.8 to 0.6 in the same depth intervals. The above findings are in agreement with Vera-Grunauer (2014) and Torres et al. (2018) who both identified soft clays with diatoms in the upper 15-20 m in Guayaquil Bay. However, direct measurements of diatom content are not available at the Murano site, and therefore further research studies are necessary to confirm this hypothesis;
- In terms of permeability, the CPTu and DMT dissipation tests are in broad agreement with the k estimations obtained from I_c . The upper 15 m-layer revealed slightly higher values when compared to the permeability of the layer between 15 and 30 m depth, potentially associating this behavior to the porous shape of diatoms, more abundant in the top clayey layer;
- The comparison between predicted and measured V_s values suggested that DMT prediction is more reliable

than CPT and SPT predictions. The high number of V_s correlations developed for CPT and SPT test detected a wide variability within the V_s profile of the soft clays, having estimates up to two-four times the measured values. The arisen uncertainty could be due to the dependency to numerous and different parameters related to the geological age, soil type and in situ stress state that CPT and SPT parameters may not capture correctly. At the same time, DMT (through K_D) is well correlated by a single correlation to stress history, prestraining/aging and structure scarcely felt by q_c and N_{SPT} (Amoroso, 2014);

- The nonlinear soil behavior of the soft clays at Murano site was presented by means of literature data and direct SDMT data interpretation. The $G/G_0-\gamma$ decay curves in the estuarine deltaic clays (zone D3) resulted in good agreement using SDMT and cyclic triaxial tests, identifying a similar behavior in the curves of upper 15.5 m, while the deeper $G/G_0-\gamma$ curves decay much faster. The behavior of the curves resulted related to the higher values of K_D , and hence of OCR and K_θ , detected for the upper layer, confirming a possible relationship with the different concentration of diatoms. The use of SDMT in estimating stiffness decay curves could be therefore advantageous for the geotechnical design, although further investigation is needed to better understand the influence of diatoms content on decay curves.

Acknowledgements

Special thanks to Studio Prof. Marchetti (Italy) for kindly providing the SDMT apparatus and to Prof. Maurizio Mulas (Escuela Superior Politécnica del Litoral, Ecuador) for sharing scientific geological information of the studied area.

Declaration of interest

The authors declare that they have no known competing financial interests or personal relationships that could have appeared to influence the work reported in this paper.

Authors' contributions

Bosco Intriago Álvarez: conceptualization, data curation, formal analysis, writing – original draft. Hernán Bazurto Palma: conceptualization, formal analysis, writing – original draft. Davide Besenon: formal analysis, funding acquisition, investigation, methodology, writing – review & editing. Xavier Vera-Grunauer: supervision, validation, investigation, writing – review & editing. Sara Amoroso: conceptualization, methodology, investigation, supervision, validation, writing – review & editing.

List of symbols

ASF	Age scaling factor
C_E	Energy correction factor
c_h	Consolidation in horizontal direction
$CPTu$	Cone penetration test with pore pressure measurement – piezocone test.
c_v	Consolidation in vertical direction
DMT	Flat Dilatometer Test
E_D	Dilatometer modulus
f_s	Sleeve friction resistance
g	Gravity
G	Shear modulus
G_{DMT}	Working strain shear modulus
GWT	Ground water level
G_0	Small strain shear modulus
I_c	Soil behavior type index
I_D	Material index
I_L	Liquidity index
I_P	Plasticity index
k	Coefficient of permeability
K_D	Horizontal stress index
k_h	Horizontal coefficient of permeability
k_v	Vertical coefficient of permeability
K_0	In situ earth pressure coefficient
M	Constrained modulus
MAM	Microtremor Array Measurement
$MASW$	Multichannel Analysis of Surface Waves
M_{DMT}	Constrained modulus (DMT)
NC	Normally consolidated
N_{kc}	Vera-Grunauer (2014) correlation factor
$N_{kt} S_u$	reduction factor
N_{SPT}	SPT blow counts
N_{60}	Energy corrected SPT blow count
OCR	Over Consolidation Ratio
p_a	Atmospheric pressure
p_0	Corrected first DMT reading
p_l	Corrected DMT second reading
q_c	Cone resistance
q_t	Corrected cone resistance
R_f	Friction ratio
$SDMT$	Seismic Dilatometer Test
SF	Scaling factor
$SHANSEP$	Stress History and Normalized Soil Engineering Properties
S,m	Vera-Grunauer (2014) parameters site
SPT	Standard Penetration Test
s_u	Undrained shear strength
t	Time in the dissipation test
Te	Elastic period
t_{flex}	Contraflexure point in the dissipation curve
TI	Trinitaria Island
t_{50}	Time for the 50% of the dissipation
$USCS$	Unified Soil Classification System
u_0	Hydrostatic pore water pressure

u_2	Pore water pressure at base of sleeve
V_s	Shear wave velocity
w	Water content
w_L	Liquid limit
w_P	Plastic limit
Z	Depth
β	Ratio between undrained shear strength and effective vertical stress
γ	Total unit weight / shear strain
γ_{DMT}	Shear strain associated with the working strain DMT modulus
γ_s	Volumetric weight
ρ	Density
σ'_{h0}	Horizontal effective stress
σ'_{v0}	Vertical effective stress
σ_{v0}	Total vertical stress
ν	Poisson's constant

References

- Akin, M.K., Kramer, S.L., & Topal, T. (2011). Empirical correlations of shear wave velocity (V_s) and penetration resistance (SPT-N) for different soils in an earthquake-prone area (Erbaa-Turkey). *Engineering Geology*, 119(1-2), 1-17. <http://dx.doi.org/10.1016/j.enggeo.2011.01.007>.
- Amoroso, S. (2014). Prediction of the shear wave velocity V_s from CPT and DMT at research sites. *Frontiers of Structural and Civil Engineering*, 8(1), 83-92. <http://dx.doi.org/10.1007/s11709-013-0234-6>.
- Amoroso, S., Monaco, P., Lehane, B., & Marchetti, D. (2014). Examination of the potential of the seismic dilatometer (SDMT) to estimate in situ stiffness decay curves in various soil types. *Soils and Rocks*, 37(3), 177-194.
- Andrus, R.D., Mohanan, N.P., Piratheepan, P., Ellis, B.S., & Holzer, T.L. (2007). Predicting shear-wave velocity from cone penetration resistance. In *Proceedings of the 4th International Conference on Earthquake Geotechnical Engineering: Vol. 2528*. Thessaloniki. Springer.
- ASTM D2487. (2017). *Standard Classification of Soils for Engineering Purposes (Unified Soil Classification System)*. ASTM International, West Conshohocken, PA.
- Baligh, M.M., & Scott, R.F. (1975). Quasi-static deep penetration in clays. *Journal of Geotechnical and Geoenvironmental Engineering*, 101(11), 1119-1133.
- Benítez, S., Álvarez, V., Vera-Grunauer, X., & Mera, W. (2005). *Geological study of Guayaquil city*. UCSG.
- Benítez, S.B. (1990). Stratigraphy of the Cayo and Guayaquil formations in the Chongón-Colonche Cordillera: towards a redefinition. *Geociencias*, 3, 7-11. [in Spanish].
- Benítez, S.B. (1995). Geodynamic evolution of the south Ecuadorian coastal province in the upper tertiary cretaceous. *Geologie Alpine*, 71, 3-163. [in French].
- Berisavljević, D. (2017). *Geotechnical soil modeling based on the parameters obtained by seismic* [PhD thesis]. University of Belgrade at Serbia.

- Boncio, P., Amoroso, S., Galadini, F., Galderisi, A., Iezzi, G., & Liberi, F. (2020). Earthquake-induced liquefaction features in a late quaternary fine-grained lacustrine succession (Fucino Lake, Italy): implications for microzonation studies. *Engineering Geology*, 272, 105621. <http://dx.doi.org/10.1016/j.enggeo.2020.105621>.
- Bouckovalas, G., Kalteziotis, N., Sabatakakis, N., & Zervogiannis, C. (1989). Shear wave velocity in a very soft clay-measurements and correlations. In *Proceedings of the 12th International Conference Soil Mechanics Foundation Engineering (ICSMFE)* (pp. 191-194). Rotterdam: A.A. Balkema Publishers.
- Brown, T., & Hettiarachchi, H. (2008). Estimating shear strength properties of soils using SPT blow counts: an energy balance approach. In *GeoCongress 2008: Characterization, Monitoring, and Modeling of GeoSystems* (pp. 364-371). Reston, VA: ASCE. [http://dx.doi.org/10.1061/40972\(311\)46](http://dx.doi.org/10.1061/40972(311)46).
- Caicedo, B., Mendoza, C., López, F., & Lizcano, A. (2018). Behavior of diatomaceous soil in lacustrine deposits of Bogotá, Colombia. *Journal of Rock Mechanics and Geotechnical Engineering*, 10(2), 367-379. <http://dx.doi.org/10.1016/j.jrmge.2017.10.005>.
- Chunga, K., Ochoa-Cornejo, F., Mulas, M., Toulkeridis, T., & Menéndez, E. (2019). Characterization of geological faults related to cortical earthquakes of Guayaquil Gulf (Ecuador). *Andean Geology*, 46(1), 66-81. [in Spanish]
- Di Mariano, A., Amoroso, S., Arroyo, M., Monaco, P., & Gens, A. (2019). SDMT-based numerical analyses of deep excavation in soft soil. *Journal of Geotechnical and Geoenvironmental Engineering*, 145(1), 04018102. [http://dx.doi.org/10.1061/\(asce\)gt.1943-5606.0001993](http://dx.doi.org/10.1061/(asce)gt.1943-5606.0001993).
- Díaz-Rodríguez, J.A., & González-Rodríguez, R.R. (2013). Influence of diatom microfossils on soil compressibility. In *Proceedings of the International XVIII Conference on Soil Mechanics and Geotechnical Engineering* (pp. 325-328). Presses des Ponts, CFMS & ISSMGE.
- Dikmen, Ü. (2009). Statistical correlations of shear wave velocity and penetration resistance for soils. *Journal of Geophysics and Engineering*, 6(1), 61-72.
- Egüez, A., Alvarado, A., Yepes, H., Machette, M.N., Costa, C.H., Dart, R.L., & Bradley, L.A. (2003). Database and map of Quaternary faults and folds of Ecuador and its offshore regions. In US Geological Survey. *US Geological Survey Open-File Report*. US Geological Survey.
- Fabbrocino, S., Lanzano, G., Forte, G., de Magistris, F.S., & Fabbrocino, G. (2015). SPT blow count Vs. shear wave velocity relationship in the structurally complex formations of the Molise Region (Italy). *Engineering Geology*, 187, 84-97.
- Hegazy, Ya., & Mayne, Pw. (1995). Statistical correlations between V_s and cone penetration data for different soil types. In *Proceedings of the International Symposium on Cone Penetration Testing, CPT* (pp. 173-178). Linköping. SGS.
- Holtz, R.D., Kovacs, W.D., & Sheahan, T.C. (1981). *An introduction to geotechnical engineering*. Prentice Hall.
- Imai, T., & Yoshimura, Y. (1970). Elastic wave velocity and soil properties in soft soil. *Tsuchito-Kiso*, 18(1), 17-22. [in Japanese]
- Iyisan, R. (1996). Correlations between shear wave velocity and in-situ penetration test results. *Teknik Dergi*, 7, 371-374. [in Turkish]
- Jamiolkowski, M., Ghionna, V.N., Lancellotta, R., & Pasqualini, E. (1988). New correlations of penetration tests for design practice. In *Proceedings of the International Symposium on penetration testing; ISOPT-1* (pp. 263-296). Rotterdam: A.A. Balkema Publishers.
- Jinan, Z. (1987). Correlation between seismic wave velocity and the number of blow of SPT and depth. *Chinese Journal of Geotechnical Engineering*, 92-100.
- Kalteziotis, N., Sabatakakis, N., & Vassiliou, J. (1992). Evaluation of dynamic characteristics of Greek soil formations, In *Second Hellenic Conference on Geotechnical Engineering* (pp. 239-246). Conference on Geotechnical Engineering (in Greek).
- Kulhawy, F.H., & Mayne, P.W. (1990). *Manual on estimating soil properties for foundation design*. Electric Power Research Inst.
- Look, B.G. (2007). *Handbook of geotechnical investigation and design tables*. CRC Press/Balkema.
- Losic, D., Pillar, R.J., Dilger, T., Mitchell, J.G., & Voelcker, N.H. (2007). Atomic force microscopy (AFM) characterization of the porous silica nanostructure of two centric diatoms. *Journal of Porous Materials*, 14(1), 61-69.
- Lunne, T., Berre, T., & Strandvik, S. (1997). Sample disturbance effects in soft low plastic Norwegian clay. In *Proceedings of the Conference on Recent Developments in Soil and Pavement Mechanics* (pp. 81-102). Rotterdam: A.A. Balkema Publishers.
- Madiari, C., & Simoni, G. (2004). Shear wave velocity-penetration resistance correlation for Holocene and Pleistocene soils of an area in central Italy. In *Proceedings of the 2nd International Conference on Geotechnical Site Characterization (ISC'2)* (pp. 687-1694). Amsterdam: IOS Press.
- Marchetti, S. (1980). In situ tests by flat dilatometer. *Journal of the Geotechnical Engineering Division*, 106(3), 299-321.
- Marchetti, S., & Crapps, D.K. (1981). *Flat dilatometer manual*. Schmertmann and Crapps Inc.
- Marchetti, S., & Totani, G. (1989). Ch evaluation from DMTA dissipation curves. In *Proceedings of the 12th International Conference on Soil Mechanics and Foundation Engineering* (pp. 281-286). Rio de Janeiro, A.A. Balkema Publishers.
- Marchetti, S., Monaco, P., Totani, G., & Calabrese, M. (2001). The flat dilatometer test (DMT) in soil investigations. In *Proceedings of the 2nd International Flat Dilatometer Conference* (pp. 7-48). Reston, VA: ASCE. ISSMGE committee TC16.
- Marchetti, S., Monaco, P., Totani, G., & Marchetti, D. (2008). In situ tests by seismic dilatometer (SDMT). In *Proceedings of the From Research to Practice in*

- Geotechnical Engineering* (pp. 292-311). Reston, VA: ASCE. [https://doi.org/10.1061/40962\(325\)7](https://doi.org/10.1061/40962(325)7).
- Mayne, P.W. (2001). Stress-strain-strength-flow parameters from enhanced in-situ tests. In *Proceedings of the International Conference on In Situ Measurement of Soil Properties and Case Histories* (pp. 27-47). Bali.
- Mayne, P.W. (2005). Unexpected but foreseeable mat settlements on Piedmont residuum. *ISSMGE International Journal of Geoenvironmental Case Histories*, 1(1), 5-17.
- Mayne, P.W. (2006). In-situ test calibrations for evaluating soil parameters. In *Proceedings of the 2nd International Workshop on Characterization and Engineering Properties of Natural Soils* (pp. 1601-1652). London: Taylor & Francis Group.
- Mayne, P.W. (2007). *Cone penetration testing state-of-practice* (NCHRP Project 20-05). Transportation Research Board.
- Mayne, P.W. (2016). Evaluating effective stress parameters and undrained shear strengths of soft-firm clays from CPT and DMT. *Australian Geomechanics Journal*, 51(4), 27-55.
- Mayne, P.W., Coop, M.R., Springman, S., Huang, A.-B., & Zornberg, J. (2009). Geomaterial behavior and testing. In *Proceedings of the 17th International Conference on Soil Mechanics and Geotechnical Engineering* (pp. 2777-2872). Rotterdam, The Netherlands: IOS Press.
- Monaco, P., & Calabrese, M. (2006). DMT-Predicted Vs. Observed Settlements: A Review of the Available Experience. In *Proceedings of the 2nd International Conference on Flat Dilatometer* (pp. 244-252). Washington, D.C.
- Monaco, P., Amoroso, S., Marchetti, S., Marchetti, D., Totani, G., Cola, S., & Simonini, P. (2014). Overconsolidation and stiffness of Venice lagoon sands and silts from SDMT and CPTU. *Journal of Geotechnical and Geoenvironmental Engineering*, 140(1), 215-227. [http://dx.doi.org/10.1061/\(ASCE\)GT.1943-5606.0000965](http://dx.doi.org/10.1061/(ASCE)GT.1943-5606.0000965).
- Nagase, H., Shimizu, K., Hiro-Oka, A., Tanoue, Y., & Saitoh, Y. (2006). Earthquake-induced residual deformation of Ariake clay deposits with leaching. *Soil Dynamics and Earthquake Engineering*, 26(2-4), 209-220.
- Ohsaki, Y., & Iwasaki, R. (1973). On dynamic shear moduli and Poisson's ratios of soil deposits. *Soil and Foundation*, 13(4), 61-73.
- Parez, L., & Fauriel, R. (1988). The piezocone improvements made to soil recognition. *Revue Française de Géotechnique*, 13-27 (in French).
- Robertson, P.K. (2009). Interpretation of cone penetration tests—a unified approach. *Canadian Geotechnical Journal*, 46(11), 1337-1355.
- Robertson, P.K. (2010). Estimating in-situ soil permeability from CPT & CPTu. In *Memorias Del 2nd International Symposium on Cone Penetration Testing*. Pomona, California: California State Polytechnic University.
- Robertson, P.K. (2012). Discussion of Influence of particle size on the correlation between shear wave velocity and cone tip resistance. *Canadian Geotechnical Journal*, 49(1), 121-123.
- Robertson, P.K., & Cabal, K.L. (2015). *Guide to cone penetration testing for geotechnical engineering* (6th ed.). Gregg Drilling and Testing Inc.
- Robertson, P.K., Sully, J.P., Woeller, D.J., Lunne, T., Powell, J.J.M., & Gillespie, D.G. (1992). Estimating coefficient of consolidation from piezocone tests. *Canadian Geotechnical Journal*, 29(4), 539-550. <http://dx.doi.org/10.1139/t92-061>.
- Rodríguez, J.F., Auvinet, G., & Martínez, H.E. (2015). Settlement analysis of friction piles in consolidating soft soils. *DYNA Journal Engineering*, 82(192), 211-220. <https://doi.org/http://dx.doi.org/10.15446/dyna.v82n192.47752>.
- Salocchi, A.C., Minarelli, L., Lugli, S., Amoroso, S., Rollins, K.M., & Fontana, D. (2020). Liquefaction source layer for sand blows induced by the 2016 megathrust earthquake (Mw 7.8) in Ecuador (Boca de Briceño). *Journal of South American Earth Sciences*, 103, 102737.
- Schmertmann, J.H. (1986). Dilatometer to compute foundation settlement. In *Proceedings of the In Situ* (pp. 303-321). Gainesville, FL: Schmertmann & Crapps Inc.
- Schmertmann, J.H. (1988). Dilatometers settle in. *Civil Engineering*, 58(3), 68.
- Shiwakoti, D.R., Tanaka, H., Tanaka, M., & Locat, J. (2002). Influences of diatom microfossils on engineering properties of soils. *Soil and Foundation*, 42(3), 1-17.
- Simonini, P., & Cola, S. (2000). Use of piezocone to predict maximum stiffness of Venetian soils. *Journal of Geotechnical and Geoenvironmental Engineering*, 126(4), 378-382.
- Stroud, M.A. (1988). The standard penetration test—its application and interpretation. In *Conference on Penetration Testing in the UK*. London: Thomas Telford.
- Teachavorasinskun, S., Thongchim, P., & Lukkunaprasit, P. (2002). Shear modulus and damping of soft Bangkok clays. *Canadian Geotechnical Journal*, 39(5), 1201-1208.
- Teh, C.I., & Houlsby, G.T. (1991). An analytical study of the cone penetration test in clay. *Geotechnique*, 41(1), 17-34. <http://dx.doi.org/10.1680/geot.1991.41.1.17>.
- Torres, G., Recalde, S., Narea, R., Troccoli, L., & Rentería, W. (2018). Spatio-temporal variability of phytoplankton and oceanographic variables in El Golfo de Guayaquil during 2013-15. *Revista del Instituto de Investigación de la Facultad de Ingeniería Geológica, Minera, Metalúrgica y Geográfica*, 20(40), 70-79. [in Spanish].
- Vera-Grunauer, X. (2014). *Seismic response of a soft, high plasticity, diatomaceous naturally cemented clay deposit* [PhD thesis]. University of California at Berkeley.
- Wair, B.R., DeJong, J.T., & Shantz, T. (2012). *Guidelines for Estimation of Shear Wave Velocity Profiles*. Pacific Earthquake Engineering Research Center.
- Yu, H.-S. (2004). James K. Mitchell Lecture. In situ soil testing: from mechanics to interpretation. In *Proceedings of the 2nd International Conference on Geotechnical Site Characterization (ISC'2)* (pp. 3-38). Rotterdam, Netherlands: Millpress.